Gemi ve Deniz Teknolojisi
Sayı: 222, Aralık 2022
ISSN: 1300-1973, e-ISSN: 2651-530X, Dergi ana sayfası: http://www.gmoshipmar.org/
Araştırma Makalesi

Tank Geometrisinin Çalkantı Kuvvetlerine Etkisi

Fatih Cüneyd Korkmaz

Gemi Makineleri İşletme Mühendisliği Bölümü, Gemi İnşaatı ve Denizcilik Fakültesi, Yıldız Teknik Üniversitesi, İstanbul, Türkiye

fkorkmaz@yildiz.edu.tr, ORCID: 0000-0001-9250-5265

ÖZET

Çalkantı kuvvetlerinin değişiminde dalga formu kadar, çarpma yüzeyinin geometrisi de etkilidir. Dalga form ise çalkantı hareketinde; tankın şekline, salınım frekansının tankın doğal frekanslarıyla çakışmasına bağlı olarak değişir. Bu çalışmada benzer boyuttaki dikdörtgen ve pahlı tankın aynı salınım frekansındaki tek eksende salınım esnasında meydana gelen yüzey deformasyonları ve yanal yüzeylerde oluşturduğu basınçların karşılaştırılması yapılmıştır. Geniş salınım frekans aralığındaki çalkantı sebebiyle yüzeylerde oluşan basınç dağılımı her iki tank için ölçülmüştür. Serbest yüzey deformasyonları rezonans ve rezonans dışı bölgelerde takip edilerek dalgaların çarpma etkileri karşılaştırılmıştır. Her iki tankta da rezonans bölgelerinde maksimum basınçlar ölçülürken diğer salınım frekanslarında basınçlar düşmüştür. Tankların benzer salınım-doğal frekans oranlarındaki çalkantıları, pahlı tankın geometrisi yardımıyla dalga formlarını değiştirdiği gibi aynı basınç ölçüm noktalarında da daha az ölçülmesi sebep olmuştur.

Anahtar kelimeler: Sıvı Çalkantısı, dikdörtgen tank, pahlı tank, basınç ölçümü, serbest yüzey takibi

Makale Geçmişi: Geliş 20/10/2022 – Kabul 13/12/2022

https://doi.org/10.54926/gdt.1192083

GMO Journal of Ship and Marine Technology
Issue: 222, December 2022
ISSN: 1300-1973, e-ISSN: 2651-530X, Journal homepage: http://www.gmoshipmar.org/
Research Article

The Effect of Tank Geometry on Sloshing Forces

Fatih Cüneyd Korkmaz

Department of Marine Engineering Operations, Naval Architecture and Maritime Faculty, Yıldız Technical University, Istanbul, Türkiye

fkorkmaz@yildiz.edu.tr, ORCID: 0000-0001-9250-5265

ABSTRACT

The geometry of the impact surface is as effective as the wave shape in the change of sloshing forces. The wave shape depends on the shape of the tank, oscillation frequency coinciding with the natural frequencies of the tank under sloshing motion. This study compares the surface deformations and pressures on the lateral walls that occur during oscillation along one axis at the same oscillation frequency between a rectangular tank and a chamfered tank of similar dimensions. The pressure distribution on the surfaces due to sloshing was measured for both tanks over a wide range of oscillation frequencies. From experiments, free surface deformations were monitored in the resonant and non-resonant regions, and the impact effects of the waves were compared. While maximum pressures were measured in the resonant regions of both tanks, pressures decreased at other oscillation frequencies. The sloshing of the tanks changed the wave shapes based on the geometry of the chamfered tank and also caused lower measurements at the same pressure measurement points at similar oscillation/natural frequency ratios.

Keywords: Liquid sloshing, rectangular tank, chamfered tank, pressure measurement, free surface tracking

Article History: Received 20/10/2022 – Accepted 13/12/2022

ISSN: 1300-1973, e-ISSN: 2651-530X, Dergi ana sayfası: http://www.gmoshipmar.org/
Araştırma Makalesi

1. Introduction

Sloshing is a phenomenon that causes internal forces by deforming the free surface of the liquid as a result of energy transferring from external forces to the fluid inside a tank. Measuring and estimating sloshing forces are important in terms of the possible damage to a tank's inner walls and disrupting the stability of the container. In addition, various wave types and the geometry of the impact points result in a story that differs from the physical point of view. Some studies are found to have measured or numerically approximated the pressure distribution under sloshing motion in different geometrically shaped tanks. Lee et al. (2007) performed a numerical analysis to evaluate the effect of air trapped in the wave crest during sloshing in LNG tanks. The effects from fill levels and waveforms during horizontal oscillation have also been discussed. Some wave forms create serious impacts when hitting the tank walls. Bullock et al. (2007) investigated the effects from four wave types on vertical and sloping walls at various angles. Kısacık et al. (2012) investigated the effect of extreme waves on a vertical wall and displayed the pressure distributions along the wall. Lugni et al. (2010) investigated the impact dynamics from various forms of wave strikes using different ullage pressure values inside the tank. Chella et al. (2012) investigated the impact from waves breaking on offshore structures. Cuomo et al. (2010,2011) studied the effects from waves breaking on coastal structures. Graczyk and Moan (2008) focused on the duration until maximum pressure is reached in LNG tanks under sloshing motion. Nasar et al. (2009) conducted an experimental study to understand the sloshing effect in a modeled tank exposed to irregular waves. The pressures on the walls were measured for tanks of different geometries under the same oscillation frequencies. Al Mashan et al. (2021) studied wave impacts on offshore structures. Souto-Iglesias and Botia-Vera (2012) investigated and monitored fluid motions due to sloshing by measuring the impacts in a rectangular tank. Ding et al. (2020) investigated the effect of liquid sloshing on LNG tanks under various loads. Song et al. (2013) studied liquid sloshing in a partially filled rectangular tank and experimentally discussed the effects from waves on the walls.

Sloshing forces for fluids with different viscosities will vary even under the same oscillation frequency of excitation of a tank. Zou et al. (2015) studied the effects of viscosity with regard to sloshing forces. Forces with lower impacts on the sidewalls have been proven with regard to high-viscosity fluids due to higher energy losses from viscous friction. Souto-Iglesias et al. (2015) investigated the role of tank width with regard to harmonic oscillation to experimentally study the possible change in pressure values. Kim et al. (2017) experimentally investigated the scale effect on sloshing and noted that the position of maximum pressure changes in a scaled tank. Tosun et al. (2017) used an image processing method to estimate the sloshing forces by monitoring free surface deformations. Lu et al. (2018) conducted a series of experiments to examine sloshing at various liquid fill levels. Their study showed the free surface to exhibit different deformations based on the varying natural frequencies at each fluid level.

Another research area has focused on reducing sloshing forces. Some researchers have attempted to absorb fluid forces by adding additional structures to the tank interior. Xue et al. (2017) investigated how to reduce sloshing forces by adding porous partitions to LNG tanks and discussed the effects from various modifications with regard to porous partitions. Lee et al. (2021) investigated the sloshing effect on Type C tanks with internal structural members. Korkmaz and Güzel (2021) conducted research to find the optimum number of obstacles with regard to slosh reduction by using perforated partitions in rectangular tanks. Another approach for reducing sloshing motion involves damping the free surface level by adding floating bodies to the tank (Sauret et al., 2015). In addition, some new studies have investigated the impacts from layered fluids as a different proposition. Korkmaz (2022) showed the

effectiveness of applying a high viscosity fluid as a second layer in order to mitigate the sloshing impact from a low viscosity fluid as the first layer.

Additionally, the effects of air bubbles have been widely discussed regarding wave breaking scenarios. The general tendency indicates compressed air to reduce the impact effects, with recent studies making more detailed comments. Bredmos et al. (2009) examined the effects of trapped air on the impact from waves breaking along the vertical wall. Bredmos et al. (2015) also studied the impact of aeration regarding various types of waves using analytical and numerical methods. They reported impact loads to have less of an effect on the structure due to air bubbles at the crest of the wave. Lugni et al. (2010) stated the effects of trapped air to change depending on cavitation. Higher pressures were measure when cavitation overlaps the oscillation frequency. However, they also mentioned a large volume bubble trapped under the wave crest to act as an air cushion between the wall and the fluid, measuring lower pressures.

It is observed that from literature, sloshing impact data on one type of geometries are convincing. More than one type of tanks are scarce. The current study investigates sloshing loads using two different tank geometries at the same fill levels and oscillation frequencies. The tap water was chosen as experimental fluids. The pressure distributions on the lateral surfaces of the rectangular and chamfered tanks were investigated under horizontal oscillatory motions. Free surface deformations were monitored, and the impact effects of the waveforms were discussed with regard to both tanks. The 16 different horizontal oscillation frequencies of the tank were studied and were varied enough to include the primary natural frequency of the tank while examining sloshing loads at resonant and non-resonant frequencies.

2. Experimental Setup

In this work, sloshing event inside of a rectangular and chamfered tanks by a horizontal oscillation were investigated experimentally. The amplitude of each tank's horizontal movement was kept constant while giving different sloshing motions to the tanks by changing the forcing frequency in the experiments. The effects from different waveforms on the lateral surfaces were measured. The tanks were made by attaching transparent acrylic sheets of different sizes (see Figure 1). The tanks were kept narrow to focus on two-dimensional effects. A hole was provided for the top plate of both tanks to maintain atmospheric pressure conditions and also to ensure that the water level of the tank remained constant during heavy turbulence. The tanks were mounted on a table able to move along a single axis. The oscillating motion was supplied with a sinusoidal law:

$$X(t) = a_n \sin \omega t \tag{1}$$

where a_n is the amplitude of the tank movement, ω is the oscillation frequency, and t is time. The oscillatory motion was provided by an AC motor, and the motion was transmitted to the tank through the arm mounted around the disc. Different sloshing motions were applied to the tank with a frequency inverter. The pressures were measured using pressure sensors on the side walls experiencing the sloshing. Three pressure sensors (model PCM300D SHLLJ) were mounted at different heights that can measure up to 0.4 Bars at a sensitivity of 0.5% and response time of 20 μs (50 kHz); the measured area is 3.5 mm in diameter. The measuring points for both tanks are indicated in Figure 1. The Hioki LR8400 data logger was used to record and process the data. A high-speed camera (Phantom Micro eX4) was used to monitor the free surface profiles at 800 fps. The camera was placed in front of the tank and the free surface for each fill level as the focal point. For lighting, an LED lighting panel was placed behind the tank facing the camera.

ISSN: 1300-1973, e-ISSN: 2651-530X, Dergi ana sayfası: http://www.gmoshipmar.org/
Araştırma Makalesi

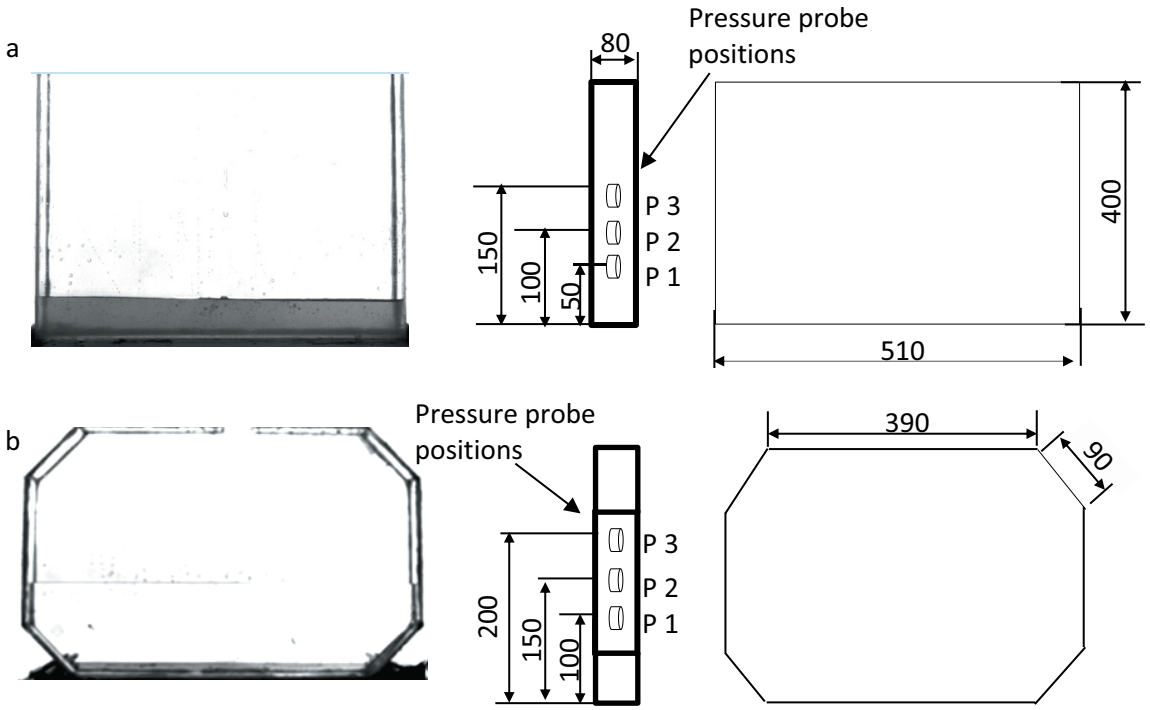

Figure 1. Draw of rectangular (a) and chamfered (b) tanks. P1, P2 and P3 represents pressure probe and attached number of sensors are positioned as ascending order from bottom to through upper side of tanks. Dimensions in mm

Sloshing forces can create significant impact loads on the tank walls, depending on how the rates of the oscillation frequency and the natural frequency of tank match one another. Two different liquid fill levels and various oscillation frequencies were applied under a constant amplitude of 11 cm (~L/4.6). The fill levels were chosen as 10 cm and 15 cm. Pressure sensors were also placed vertically in the chamfered tank. Both the pressure measurement and free surface monitoring started after the dominant oscillation frequency was reached in each experiment.

An oscillation frequency close to the tank's natural frequency is expected to create the highest free surface deformation and greatest pressure forces in the tank. The natural frequency, length L, and fill level h of a rectangular tank can be determined analytically based on Faltinsen and Timokha's (2009) following equation,

$$\omega_n^2 = g\frac{n\pi}{L}\tanh\left(\frac{n\pi}{L}h\right) \tag{2}$$

where ω_n is the natural frequency of the rectangular tank, g is gravitational acceleration, L is the length of the rectangular tank, h is the depth of the fluid, and n is the mode number. Equation (3) then provides the natural frequency correction for a chamfered tank whose chamfered parts have the dimensions (Faltinsen and Timokha, 2009):

$$\frac{\omega_n'^2}{\omega_n{}^2} = 1 - \frac{\frac{\delta_1}{\delta_2}\sinh^2\left(\pi n\frac{\delta_2}{L}\right) - \frac{\delta_1}{\delta_2}\sin^2\left(\pi n\frac{\delta_1}{L}\right)}{\pi n\sinh\left(2\pi n\frac{h}{L}\right)} \tag{3}$$

where δ_1 and δ_2 represent the horizontal and vertical dimensions of the chamfered tank and ωn' is the natural frequency of the chamfered tank. 16 oscillation frequencies were applied to the tanks in order

to understand the effects of fluid depth. Table 1 shows the details regarding fluid depths, horizontal motion frequencies, and natural frequencies for all fluid fill levels.

Table 1. Oscillation - natural frequencies for each filling levels and tanks

	Water depth (cm)	Natural Freq. ω_n (rad/s)	Natural Freq. ω_n' (rad/s)	Oscillation Frequencies (rad/s)
Case 1	10	5.75	5.71	2.8, 3.17, 3.56, 3.65, 4.07, 4.4, 4.5, 4.9, 5.06, 5.23, 5.6, 6, 6.28, 6.68, 6.97, 7.42
Case 2	15	6.63	6.6	

Figure 2 shows the pressure values taken from the same point at different times for both the rectangular and chamfered tanks in the current experiment. The repeatability of the measured pressures in the non-resonant region is high for all measurement points. The sample of P1 at the low level measurement point is selected to show in Figure 2. However, due to chaotic impact, these repeatable results might not be achieved around the resonance frequency, especially at the free surface level. For rectangular at 0.67 and chamfered at 0.68 ω/ω_n, the peak pressure values are measured with average an average uncertainty of ±1-3%. Beside that the uncertainties level may increase vicinity of resonance frequency due to high nonlinearity.

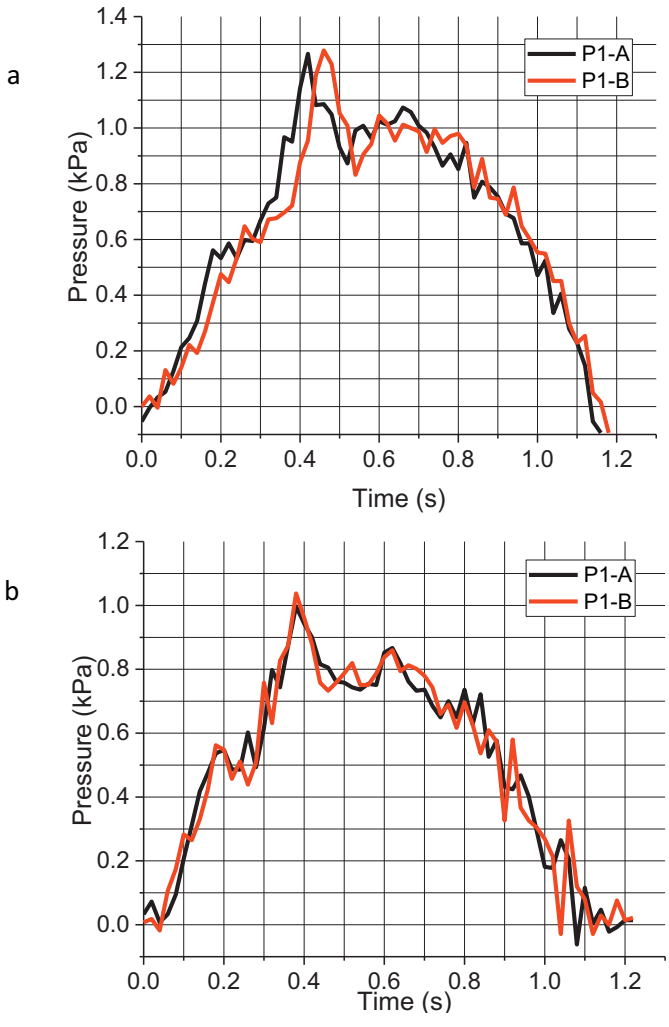

Figure 2. Repeatability of measurements at the P1 pressure sensor. A and B letter represents first and second test. Case 2 rectangular (a) at ω/ω_n=0.67 and chamfered (b) at ω/ω_n'=0.68 tank

ISSN: 1300-1973, e-ISSN: 2651-530X, Dergi ana sayfası: http://www.gmoshipmar.org/
Araştırma Makalesi

3. Results and Discussion

This section presents the experimental results for the rectangular and chamfered tanks at different oscillation frequencies. The 16 oscillation frequencies range from 2.8 rad/s to 7.42 rad/s and were applied to covering the primary natural frequencies of the tanks.

3.1 Free surface deformation

The oscillation frequency, amplitude of motion, and depth of the fluid are three main parameters affecting free surface deformations (Thiagarajan et al., 2011). Besides that the geometrical shape is another feature that effect free surface profile. For instance, the internal flow approaches until vertical wall of rectangular tank without any distortion. It causes harsh impact especially under breaking wave. However the relatively mild impact is expected at the chamfered tank. It is because, the fluid from oscillation direction, arise earlier bottom to upper side. Therefore, the incoming wave can be absorbed by interacting with the flow from the chamfered part before hitting the wall of the tank. Figure 3 shows how the same oscillation frequency was applied to both the rectangular and chamfered tanks, with the natural oscillation frequency ratios being 0.78 and 0.79 (ω/ω_n, ω/ω_n'), respectively. The free surface distribution started as a similar wave form then broke apart and deformed before the wave tip hit the side wall in the rectangular tank. The horizontal velocity of wave seems to be sufficient to break at the beginning of circle in the chamfered tank, but is obstructed to wave breaking by resultant velocity of stationary fluid at the chamfered part of tank. The difference in the tank geometries and the vertical velocity of the stationary fluid in the wave direction varied as the axial movement of the tank continued, and the two tanks showed different impacts upon their lateral surfaces. The free surface deformation was more severe because less fluid was near the resonant region at the same oscillation frequency (Figure 4).

Significant wave breaks are observed in Figure 4, especially for the rectangular tank. This wave break approached the lateral surface without being disturbed. The wave impact on the wall contained a certain amount of air, and this spread the effect of air compression over the entire surface. The results were seen to vary based on the cavitation frequency (f_r). Topliss et al. (1992) estimated the following natural frequency for two-dimensional cavitation occurring in a free surface region:

$$f_r^{\,2} = -\frac{2\gamma p}{4\pi^2 \rho r^2 \log\left(\frac{r}{2h_y}\right)} \tag{4}$$

where p is atmospheric pressure, ρ is the water density, γ is the specific heat ratio, r is the half angle of the air bubble, and h_y is the distance of the air bubble from the free surface.

The frequency of cavitation was analytically found to be ~157 rad/s under an oscillation frequency of 5.23 rad/s for case 1. Figure 5 shows in detail the impact and distribution of the air bubble under the wave tip. Contrary to the rectangular tank, the wave crest in the chamfered tank spills onto the free surface due to the wave not being able to completely break up, especially when approaching the lateral surface. Some air bubbles remained between the spilled wave and free surface. These air bubbles followed the fluid and preserved their shape without bursting or causing oscillations between the wall and the water. In the rectangular tank, however, the trapped air was clearly observed to get dispersed by the impact and turn into smaller air bubbles. The effects from the chaotic environment are transmitted toward the top of the free surface region along the lateral surface. In addition, the repeatability of the measurements is lower due to the distorted air bubbles in these regions, and the oscillation frequency was in range of the resonance region ($\omega / \omega_n = 1.099$ and $\omega / \omega_n' = 1.091$).

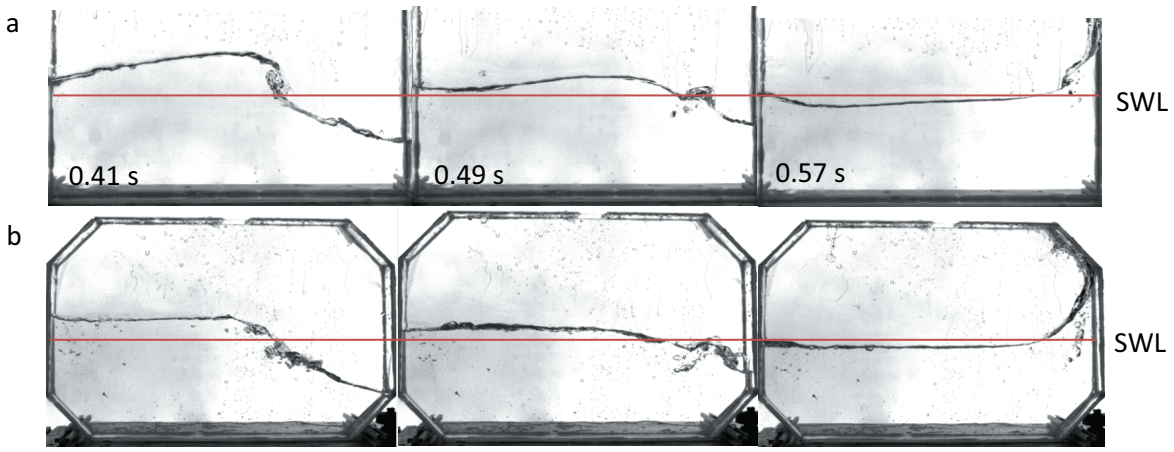

Figure 3. Free surface deformation of case 2 in rectangular (a) at ω/ω_n=1.267 and chamfered tank (b) at ω/ω_n'=1.263. SWL: Stil water level

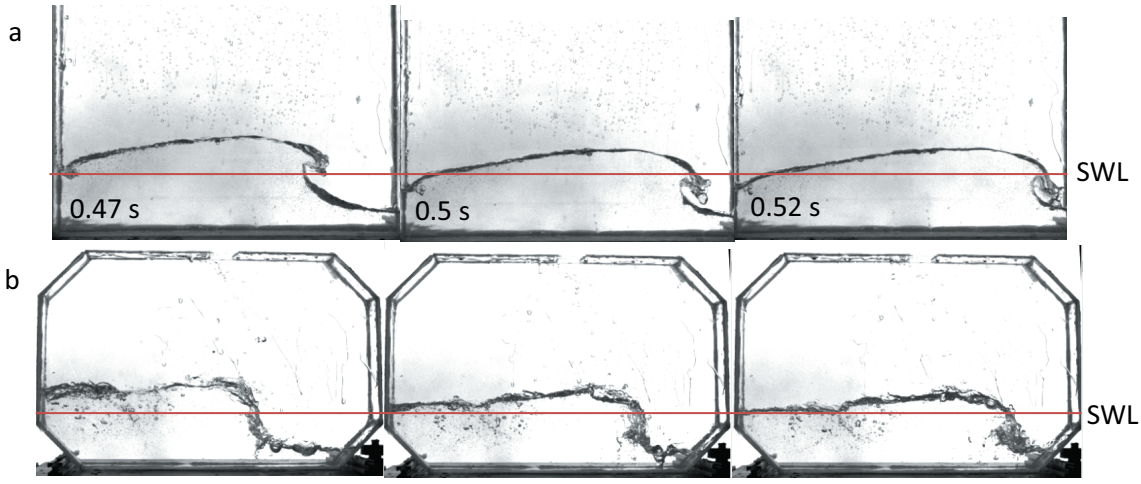

Figure 4. Free surface deformation of case 1 in rectangular (a) at ω/ω_n=1.099 and chamfered tank (b) at ω/ω_n'=1.091

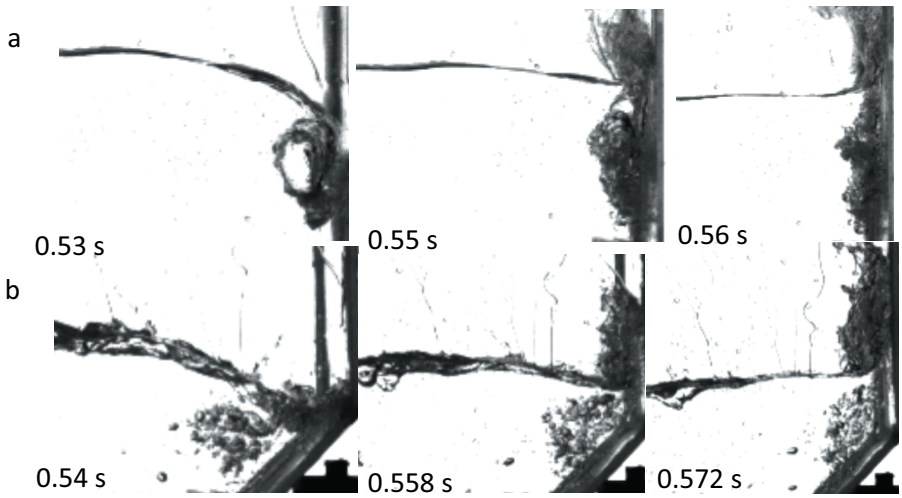

Figure 5. Close view of wave impact in case 1 under 5.23 rad/s at rectangular (a) and at chamfered tank (b)

ISSN: 1300-1973, e-ISSN: 2651-530X, Dergi ana sayfası: http://www.gmoshipmar.org/
Araştırma Makalesi

3.2 Pressure measurement

The pressures that formed on the tanks' lateral surfaces during oscillation were measured with pressure sensors. The sensors were mounted at specific heights on the flat part of the chamfered tank as well as in the rectangular tank (Figure 1). The tests were expected to show the greatest effect at the oscillation frequency for each oscillation frequency. The measured pressure values were normalized with the static pressure formula:

$$p_{static} = \rho g h \tag{5}$$

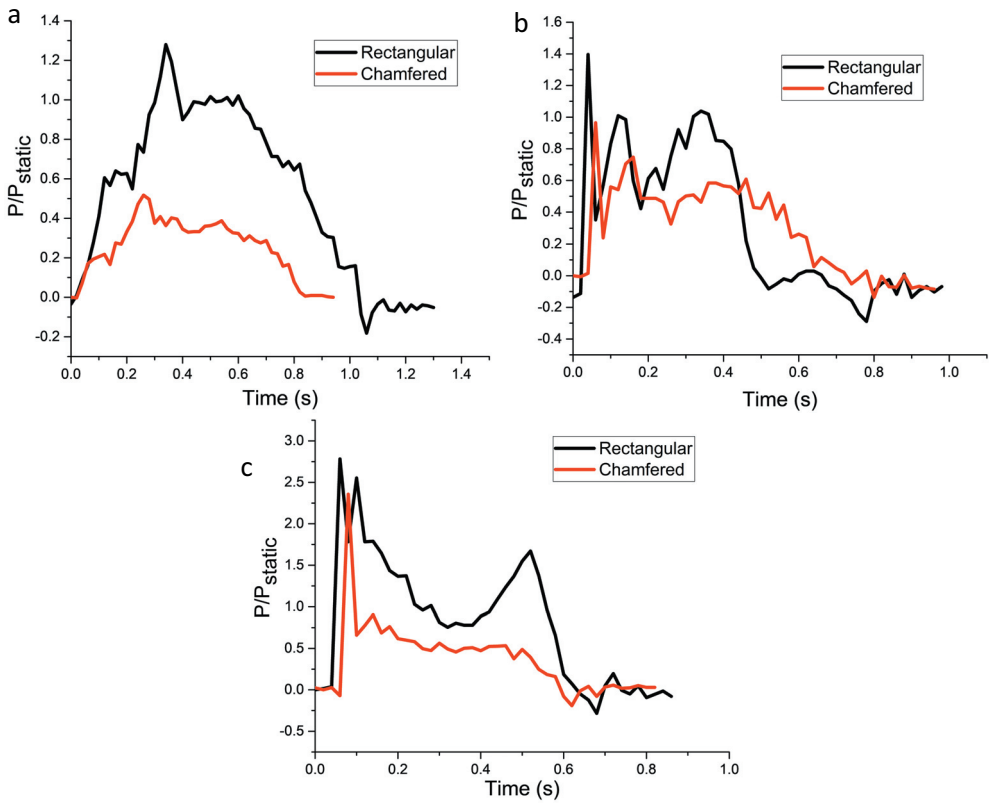

Figure 6. Pressure comparison under 4.5 (a), 5.23 (b) and 6.28 rad/s (c) oscillation frequencies for case 2 at the same measurement positions (P3 for rectangular and P2 for chamfered tank)

Figure 6 provides the results from the measurement points at the same height in both tanks for the resonance and the non-resonance regions by comparing the raw pressure values. While pressure rose gradually in the non-resonant regions (Figure 6a), the impact areas showed maximum pressure for a short period of time at the resonance region then decayed to lower pressure descending to zero (see Figure 6b & 6c). Massive pressure differences were measured between the chamfered and rectangular tanks due to the structure differences, with the chamfered tank having a pressure value under 0.68 ω/ω_n and the rectangular tank measuring 0.67 ω/ω_n. The shape of the chamfered structure mitigates and distorts the wave form's energy. However, this difference decreased and reached a maximum value in a very short time in measurements when the oscillation frequency and the natural frequencies of the tanks were closer to one another (0.78 ω/ω_n and 0.79 ω/ω_n', see Figure 6b; 0.94 ω/ω_n and 0.95 ω/ω_n', see Figure 6c). After the pressure values reached their first peak in the rectangular tank, a second peak also occurred. This shows the effect of fluid passing through a second time as it falls toward the bottom of the tank due to gravity (Zou et al., 2015). However, the pressure values remained

stable for a while and then began to decline. No second peak was clearly observed for the chamfered tank.

The average maximum pressure values on the lateral surfaces of the fluid as a result of the 16 different oscillation frequencies are shown in Figure 7. Each pressure sensor shows the maximum value in the resonance region; however, the measured pressure values showed lower impact effects as they moved away from the resonance region. The same pressure distributions were observed in both tanks, with higher values being measured at each pressure sensor at the same height in the rectangular tank while this difference was greater in the non-resonant regions compared to in the chamfered tank. Chamfered part can be seen to create much difference in the peak pressure values obtained at the P3 and P2 levels which are same positions for rectangular and chamfered tank respectively (see Figure. 17c).

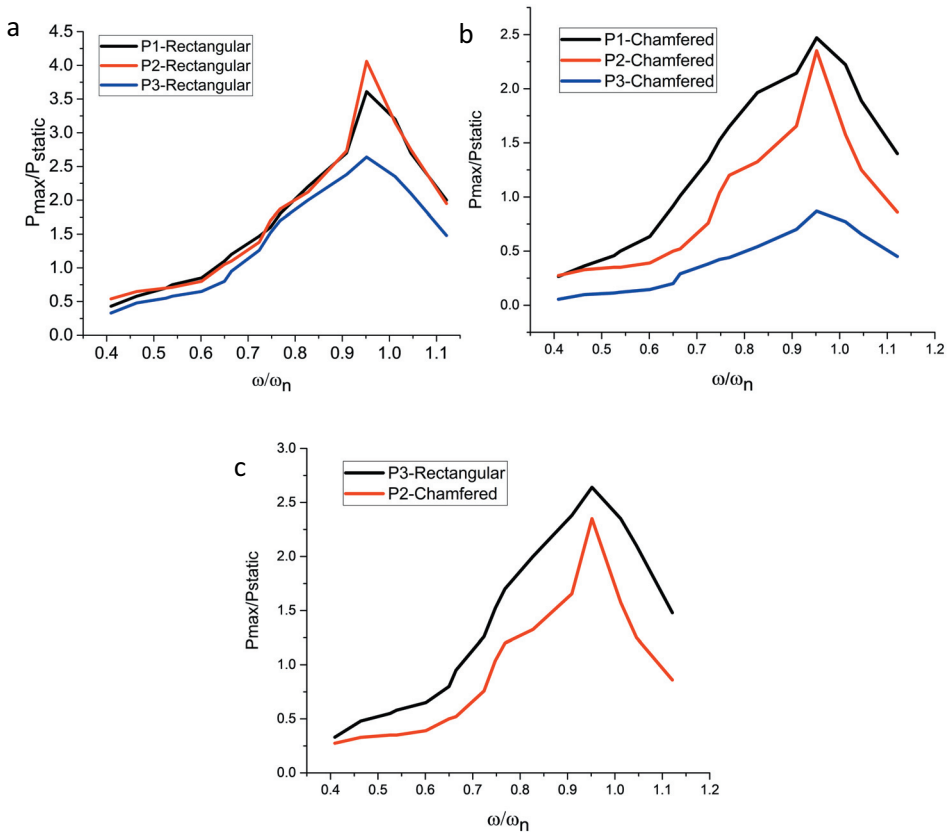

Figure 7. Peak pressure vs. excitation frequency of case 2 at the rectangular and chamfered tank

4. Conclusion

This study applied various oscillatory motions onto tanks with different geometries. The free surface deformations were monitored, and the pressure measurements on the lateral surfaces were compared, and showed the waves that formed to result in similar deformations in both tanks at the resonance frequency ratios. However, due to the geometric shape of the chamfered tank, some of the energy of the wave was dispersed through the fluid along the wave front in the chamfered section. Therefore, the chamfer tank saw the wave to affect the vertical section of the tank with less pressure. Thus, different waveforms impinged on the lateral surfaces in both tanks. The distribution of pressure intensity with respect to the resonant and non-resonant regions was similar for all measurement points in each tank. In addition, lower pressures were measured in the chamfered tank for each height compared to the rectangular tank. The measured pressure differences decreased in the resonant

regions but increased in the non-resonant regions. A more dramatic reduction of pressure distribution was observed toward the upper parts of the chamfered tank.

5. Acknowledgements

This work was supported by Research Fund of the Yildiz Technical University. Project Number: FBA-2018-3341.

6. References

AlMashan, N., Neelamani S. and Al-Houti, D. (2021). Experimental investigations on wave impact pressures under the deck and global wave forces and moments on offshore jacket platform for partial and full green water conditions. Ocean Engineering, 234, 109324.

Bredmose, H., Bullock G. N. and Hogg, A. J. (2015). Violent breaking wave impacts. Part 3. Effects of scale and aeration. J. Fluid Mech., 765, 82–113.

Bredmose, H., Peregrine D. H. and Bullock, G. N. (2009). Violent breaking wave impacts. Part 2: modelling the effect of air. J. Fluid Mech., 641, 389–430.

Bullock, G. N., Obhrai, C., Peregrine D. H. and Bredmose H. (2007). Violent breaking wave impacts. Part 1: Results from large-scale regular wave tests on vertical and sloping walls. Coastal Engineering, 54, 602–617.

Chella, M. A., Torum A. and Myrhaug, D. (2012). An Overview of Wave Impact Forces on Offshore Wind Turbine Substructures. Energy Procedia, 20, 217 – 226.

Cuomo, G., Allsop W., Bruce T. and Pearson J. (2010). Breaking wave loads at vertical seawalls and breakwaters. Coastal Engineering, 57, 424–439.

Cuomo G., Piscopia R. and Allsop W. (2011). Evaluation of wave impact loads on caisson breakwaters based on joint probability of impact maxima and rise times. Coastal Engineering, 58, 9–27.

Ding, S., Wang G. and Luo G. (2020). Study on sloshing simulation in the independent tank for an icebreaking LNG carrier. International Journal of Naval Architecture and Ocean Engineering, 12, pp. 667-679.

Faltinsen O. M. and Timokha, A. N. (2009). “Sloshing”, Cambridge University Press.

Graczyk M. and Torgeir M. (2008). A Probabilistic Assessment of Design Sloshing Pressure Time Histories in LNG Tanks. Ocean Engineering, 35 (8–9), 834–55.

Kim, S. Y., Kim, Y., Park J. J. and Kim, B. (2017). Experimental Study of Sloshing Load on LNG Tanks for Unrestricted Filling Operation. Journal of Advanced Research in Ocean Engineering, 3 (1), 041-052.

Kisacik, D., Troch P. and Van Bogaert, P. (2012). Description of loading conditions due to violent wave impacts on a vertical structure with an overhanging horizontal cantilever slab. Coastal Engineering, 60, 201–226.

Korkmaz, F. C. (2022). Damping of sloshing impact on bottom-layer fluid by adding a viscous top-layer fluid. Ocean Engineering, vol. 254, 111357.

Korkmaz, F. C., Yigit, K. and Güzel, B. (2021). Experimental Study on Sloshing Reduction Effects of Baffles. El-Cezeri , 8 (3), 1149-1157.

Lee, J., Ahn, Y., Kim, J., Kim, Y., Yang, K. K., Yi S. I. and Noh, M. H. (2021). Observation on sloshing flow and hydrodynamic pressures on cylindrical liquefied natural gas tank with swash bulkhead. Proc IMechE Part M: J Engineering for the Maritime Environment, 235 (1), 30–40.

Lee, D. H., Kim, M. H., Kwon, S. H., Kim J. W. and Lee, Y. B. (2007). A Parametric Sensitivity Study on LNG Tank Sloshing Loads by Numerical Simulations. Ocean Engineering, 34 (1), 3–9.

Lugni, C., Brocchini M. and Faltinsen, O. M. (2010). Evolution of the air cavity during a depressurized wave impact. II. The dynamic field. Physics of Fluids, 22, 056102.

Lugni, C., Miozzi, M., Brocchini M. and Faltinsen O. M. (2010). Evolution of the air cavity during a depressurized wave impact. I. The kinematic flow field. Physics of Fluids, 22, 056101.

Lu, Y., Zhou, T., Cheng, L., Zhao W. and Jiang, H. (2018). Dependence of critical filling level on excitation amplitude in a rectangular sloshing tank. Ocean Engineering, 156, 500–511.

Nasar, T., Sannasiraj S. A. and Sundar V. (2009). Wave-induced sloshing pressure in a liquid tank under irregular waves. Proceedings of the Institution of Mechanical Engineers, Part M: Journal of Engineering for the Maritime Environment, 223 (2), 145-161.

Sauret, A., Boulogne, F., Cappello, J., Dressaire E. and Stone, H. A. (2015). Damping of liquid sloshing by foams. Physics of Fluids, 27, 022103.

Song, Y. K. Chang, K. A., Ryu Y. and Kwon, S. H. (2013). Experimental study on flow kinematics and impact pressure in liquid sloshing. Exp Fluids, 54, 1592.

Souto-Iglesias, A., Botia-Vera E. and Bulian, G. (2012). Repeatability and two-dimensionality of model scale sloshing impacts. in: Proceedings of the Twenty Second International Society of Offshore and Polar Engineering Conference, Rhodes, Greece.

Souto-Iglesias, A., Bulian G. and Botia-Vera, E. (2015). A set of canonical problems in sloshing. Part 2: Influence of tank width on impact pressure statistics in regular forced angular motion. Ocean Engineering, 105, 136–159.

Thiagarajan, K. P., Rakshit D. and Repalle, N. (2011). The air–water sloshing problem: Fundamental analysis and parametric studies on excitation and fill levels. Ocean Engineering, 38, 498–508.

Topliss, M. E., Cooker M. J. and Peregrine, D. H. (1992). “Pressure oscillations during wave impact on vertical walls”. Publ by ASCE, New York, NY, United States, 2, 1639–1650.

Tosun, U., Aghazadeh, R., Sert C. and Ozer, M. (2017). Tracking free surface and estimating sloshing force using image processing. Experimental Thermal and Fluid Science, 88, 423-433.

Xue, M. A., Jiang, Z., Hu Y. and Yuan, X. (2017). Numerical Study of Porous Material Layer Effects on Mitigating Sloshing in a Membrane LNG Tank. Ocean Engineering, 218, 108240.

Zou, C. F., Wang, D. Y., Cai Z. H. and Li, Z. (2015). The effect of liquid viscosity on sloshing characteristics. J Mar Sci Technol, 20, 765–775.